

Multiscale stabilization for convection diffusion equations with heterogeneous velocity and diffusion coefficients

Eric T. Chung ^{*} Yalchin Efendiev [†] Wing Tat Leung [‡]

August 1, 2018

Abstract

We present a new stabilization technique for multiscale convection diffusion problems. Stabilization for these problems has been a challenging task, especially for the case with high Peclet numbers. Our method is based on a constraint energy minimization idea and the discontinuous Petrov-Galerkin formulation. In particular, the test functions are constructed by minimizing an appropriate energy subject to certain orthogonality conditions, and are related to the trial space. The resulting test functions have a localization property, and can therefore be computed locally. We will prove the stability, and present several numerical results. Our numerical results confirm that our test space gives a good stability, in the sense that the solution error is close to the best approximation error.

1 Introduction

In this paper, we consider a class of convection-diffusion problems in the form

$$-\nabla \cdot (\kappa \nabla u) + b \cdot \nabla u = f \quad (1)$$

with a high Peclet number, where κ is a diffusion tensor and b is a velocity vector [55, 39]. We assume that both fields contain multiscale spatial features with high contrast. There are in literature a wide range of numerical schemes for this problem that are based on constructions of special basis functions on coarse grids [29, 56, 3, 36, 32, 37, 41, 40, 31, 33, 38, 16, 30, 12, 13, 44, 34]. These methods include the Multiscale Finite Element Methods (MsFEM) [36, 32, 37, 38, 43, 2], the Variational Multiscale Methods [48, 46, 45, 6, 52, 9, 47, 23, 5, 1, 50] and the Generalized Multiscale Finite Element Method (GMsFEM) [32, 42, 43, 34, 35, 10, 21, 17, 11, 22, 19, 20]. When the above approaches are used to solve multiscale convection-dominated diffusion problems with a high Peclet number, besides finding a reduced approximate solution space, one needs to stabilize the system to avoid large errors [55]. It is known that simplified stabilization techniques do not suffice for complex problems and one needs a systematic approach to generate the necessary test spaces.

In this paper, we will derive and analyze a new stabilization technique, which combines recent developments in Constraint Energy Minimizing Generalized Multiscale Finite Element Method (CEM-GMsFEM) [18] and Discontinuous Petrov-Galerkin method (e.g., [28, 53, 54]). To motivate our method, we start with a stable fine-scale finite element discretization that fully resolves all scales of (1)

$$Au = f. \quad (2)$$

^{*}Department of Mathematics, The Chinese University of Hong Kong (CUHK), Hong Kong SAR. Email: tschung@math.cuhk.edu.hk. The research of Eric Chung is supported by Hong Kong RGC General Research Fund (Project 14317516) and CUHK Direct Grant for Research 2017-18.

[†]Department of Mathematics & Institute for Scientific Computation (ISC), Texas A&M University, College Station, Texas, USA. Email: efendiev@math.tamu.edu.

[‡]The Center for Subsurface Modeling, The Institute for Computational Engineering and Sciences, The University of Texas at Austin, Austin, TX 78712

We will apply the discontinuous Petrov-Galerkin (DPG) techniques following [24, 14, 26, 28, 25, 57] to stabilize the system. In particular, we will rewrite the above system in a mixed framework using an auxiliary variable as follows

$$Rw + Au = f, \tag{3}$$

$$A^T w = 0, \tag{4}$$

where the variable w plays the role of the test function and the matrix R is related to the norm in which we seek to achieve stability. We assume that the fine-scale system gives $w = 0$, that is, it is discretely stable. The aim of this paper is to design a space for the variable w , given a choice of the trial space for u .

Within the DPG framework, one can achieve stability by choosing test functions w with global support [4, 27]. The least squares approaches [7, 49, 8, 15] can be used to achieve stability in the natural norm. We also note that a stabilization technique based on the variational multiscale method is presented in [51]. Our goal is to design procedures for constructing test functions that are localizable and give good stability, that work well for large Peclet numbers. To construct our test functions, we assume that a given set of local multiscale trial functions is available, and that they satisfy a stable decomposition property. We note that these functions can be constructed by, for example, using the GMsFEM approach (see e.g. [32]). To find the test functions, we use the idea of CEM-GMsFEM [18]. First, we will construct an auxiliary space. In particular, for each coarse cell, we solve a spectral problem, which is defined based on the above mixed formulation (4). The first few eigenfunctions contain important features about the multiscale coefficients κ and b , and are used in the construction of our test functions. Using these local eigenfunctions and the given local trial functions, we will find the required test functions by minimizing an appropriate energy subject to some constraints. We will show that the test functions are localizable and that they give good stability of the resulting numerical scheme.

We will present some numerical results to show the performance. We will show the performance of using various coarse grid sizes and various choices of oversampling layers. We observe that, once a sufficient number of oversampling layers is used, the solution error is very close to the projection error, which is the best approximation error in the trial space. This confirms that our test space provides a good stability even for high Peclet number.

The paper is organized as follows. In Section 2, we give some basic notations and the formulation of our problem. In Section 3, we present the construction of the test space, and show that the space gives a good stability. Numerical results to validate the theory will be presented in Section 4. Finally, a conclusion is given.

2 Preliminaries

We will give some basic notations in this section. In this paper, we consider convection diffusion problems of the form

$$-\operatorname{div}(\kappa(x) \nabla u) + b(x) \cdot \nabla u = f \quad \text{in } \Omega, \tag{5}$$

subject to the homogeneous Dirichlet boundary condition $u = 0$ on $\partial\Omega$, where $\Omega \subset \mathbb{R}^d$ is the computational domain and $f \in L^2(\Omega)$ is a given source. We assume that both $\kappa(x)$ and $b(x)$ are heterogeneous coefficients with multiple scales and very high contrast, and that $b(x)$ is divergence free. We assume $\kappa_0 \leq \kappa \leq \kappa_1$ where κ_1/κ_0 is large.

We next introduce the notion of fine and coarse grids. We let \mathcal{T}^H be a usual conforming partition of the computational domain Ω into N finite elements (triangles, quadrilaterals, tetrahedra, etc.). We refer to this partition as the coarse grid and assume that each coarse element is partitioned into a connected union of fine grid blocks. The fine grid partition will be denoted by \mathcal{T}^h , and we assume that this is a refinement of the coarse grid \mathcal{T}^H . See Figure 1 for an illustration. We let N be the number of coarse elements and N_c be the number of coarse grid nodes. We remark that our test functions are defined with respect to the coarse grid, and the fine grid is used to compute the test functions numerically.

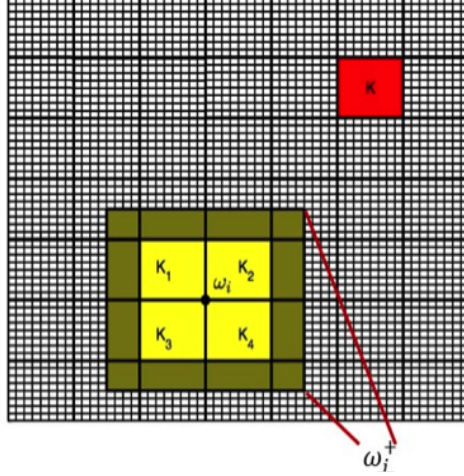


Figure 1: Illustration of the coarse grid, fine grid, coarse neighborhood and oversampling domain.

Next, we give the precise formulation of our problem. We define $V = H_0^1(\Omega)$ and the bilinear form $a : V \times V \rightarrow \mathbb{R}$ by

$$a(u, v) = \int_{\Omega} (\kappa \nabla u \cdot \nabla v + v b \cdot \nabla u).$$

Then (5) can be formulated as: find $u \in V$ such that

$$a(u, v) = (f, v), \quad \forall v \in V \quad (6)$$

where (f, v) is the $L^2(\Omega)$ inner product. In order to define our stabilization approach, we will formulate the above problem following the DPG idea as in [24, 14, 26, 28, 25, 57]. First of all, we assume that a certain trial space $V_{ms} \subset V$ is used. The trial space consists of local multiscale basis functions q_i with support on local region ω_i for the i -th coarse vertex, where the coarse neighborhood ω_i is the union of all coarse elements having the i -th vertex, see Figure 1. We remark that one can use multiple basis functions per coarse region ω_i . In addition, we assume that the trial space satisfies the following stable decomposition property:

$$\left(\sum_{i=1}^{N_c} \|u_i\|_V^2 \right)^{\frac{1}{2}} \leq C_s \|u\|_V, \quad u \in V_{ms}, \quad u = \sum_{i=1}^{N_c} u_i, \quad \text{supp}(u_i) \subset \omega_i \quad (7)$$

where $\|\cdot\|_V$ is a suitable norm which will be defined. Our main goal is to construct a suitable test space W_{ms} , so that the resulting mixed problem has a good stability property. For simplicity of our discussion, we assume that there is one basis per node. Our theory can be generalized to the case that there are multiple trial basis per node.

We will now present the DPG formulation. For each coarse element $K_i \in \mathcal{T}^H$, we define the bilinear forms

$$s^{(i)}(u, v) = \int_{K_i} \kappa \nabla u \cdot \nabla v \quad (8)$$

$$c^{(i)}(u, v) = \int_{K_i} (\kappa^{-1} |b|^2 u v + \tilde{\kappa} u v) \quad (9)$$

where $\tilde{\kappa} = \kappa \sum_{j=1}^{N_c} |\nabla \chi_j|$ and $\{\chi_j\}$ is a set of partition of unity functions corresponding to the coarse grid where the index j denotes j -th coarse vertex. Using the above bilinear forms, we define the inner product

$$(u, v)_{V_i} = s^{(i)}(u, v) + c^{(i)}(u, v) \quad (10)$$

with the associated norm $\|u\|_{V_i}^2 = s^{(i)}(u, u) + c^{(i)}(u, u)$ for the space $V(K_i)$, where we define $V(S) := H^1(S)$ and $V_0(S) := H_0^1(S)$ for a given set S . In addition, we define $(u, v)_V = \sum_{i=1}^N (u, v)_{V_i}$, which is an inner product for V . We further define

$$a^*(u, v) = a(v, u). \quad (11)$$

We next define a linear operator $T : V \rightarrow V$ by

$$a^*(Tu, v) = (u, v)_V, \quad \forall v \in V. \quad (12)$$

It is clear that T is a bijective bounded linear operator and hence T^{-1} is bounded. Using T^{-1} , we define the bilinear form r as

$$r(w, z) = (T^{-1}w, T^{-1}z)_V. \quad (13)$$

Finally, we formulate the problem as: find $(w, u) \in W_{ms} \times V_{ms}$ such that

$$r(w, z) + a(u, z) = (f, z), \quad \forall z \in W_{ms}, \quad (14)$$

$$a^*(w, v) = 0, \quad \forall v \in V_{ms}. \quad (15)$$

3 Multiscale stabilization

In this section, we will present our stabilization technique. In Section 3.1, we will give the construction of the test functions for a given choice of the trial space V_{ms} . In Section 3.2, we will give the stability analysis.

3.1 Construction of test functions

We will present the construction of the test functions. The idea is based on the CEM-GMsFEM [18]. We will first define the auxiliary space. For each coarse element $K_i \in \mathcal{T}^H$, we consider the following eigenvalue problem: find $(\lambda_j^{(i)}, \phi_j^{(i)}) \in \mathbb{R} \times V(K_i)$ such that

$$s^{(i)}(\phi_j^{(i)}, v) = \lambda_j^{(i)} c^{(i)}(\phi_j^{(i)}, v), \quad \forall v \in V(K_i). \quad (16)$$

Assume that the eigenvalues are arranged in non-decreasing order, namely $\lambda_j^{(i)} \leq \lambda_{j+1}^{(i)}$. For each K_i , we select the first J_i eigenfunctions and define the local auxiliary space $W_{aux}(K_i)$ by

$$W_{aux}(K_i) = \text{span}\{\phi_j^{(i)} \mid 1 \leq j \leq J_i\}$$

and the corresponding global auxiliary space W_{aux} by $W_{aux} = \sum_i W_{aux}(K_i)$. We remark that J_i is the number of small eigenvalues for the problem (16) and these eigenvalues typically depend on the contrast of the coefficients.

We next present the construction of the multiscale test basis functions. To do so, we define an operator $\pi : V \rightarrow W_{aux}$ by

$$\pi(u) = \sum_{i=1}^N \sum_{1 \leq j \leq J_i} \frac{1}{\lambda_j^{(i)}} \frac{c^{(i)}(u, \phi_j^{(i)})}{c^{(i)}(\phi_j^{(i)}, \phi_j^{(i)})} \phi_j^{(i)}, \quad \forall u \in V$$

where the sum with the index i denotes the sum over all coarse elements K_i . Our multiscale test space W_{ms} consists of two components W_{ms}^1 and W_{ms}^2 . We will define these two spaces as follows, and will analyze them in Section 3.2.

Now, we give the definition of the space W_{ms}^1 . For a given coarse element K_i , we consider its oversampled region K_i^+ , which is obtained by enlarging K_i by a few coarse grid cells. Then, for each $\phi_j^{(i)}$ in the auxiliary space $W_{aux}(K_i)$, we consider the following problem: find $\psi_{j,ms}^{(i)} \in V_0(K_i^+)$ such that

$$a^*(\psi_{j,ms}^{(i)}, v) + c(\pi(\psi_{j,ms}^{(i)}), \pi(v)) = c(\pi(\phi_j^{(i)}), \pi(v)), \quad \forall v \in V_0(K_i^+)$$

where the bilinear form $c = \sum_{i=1}^N c^{(i)}$. The first component of test space is defined as

$$W_{ms}^1 = \text{span}\{\psi_{j,ms}^{(i)} \mid 1 \leq j \leq J_i, 1 \leq i \leq N\}. \quad (17)$$

Next, for each trial basis function $q_i \in V_{ms}$ with support ω_i corresponding to the i -th coarse vertex, we will define a local function $\xi_i \in V_0(\omega_i)$ such that

$$a(v, \xi_i) = s(q_i, v), \quad \forall v \in V_0(\omega_i) \quad (18)$$

and we define $\eta_{i,ms} \in V(\omega_i^+)$ such that

$$a^*(\eta_{i,ms}, v) + c(\pi(\eta_{i,ms}), \pi(v)) = (q_i, v)_V - a(v, \xi_i), \quad \forall v \in V(\omega_i^+)$$

where ω_i^+ is obtained by enlarging ω_i by a few coarse cells, see Figure 1. The second component of test space is defined as

$$W_{ms}^2 = \text{span}\{\eta_{i,ms} + \xi_i \mid 1 \leq i \leq N_c\}. \quad (19)$$

Finally, our multiscale test space W_{ms} is the sum of W_{ms}^1 and W_{ms}^2 .

3.2 Stability analysis

We will analyze the stability in this section. We first notice that the test functions defined in (17) and (19) have local supports. This is the result of a localization property of a related space W_{glo} , which contains functions defined globally. The space W_{glo} also consists of two components W_{glo}^1 and W_{glo}^2 . To define the space W_{glo}^1 , we find $\psi_j^{(i)} \in V$ such that

$$a^*(\psi_j^{(i)}, v) + c(\pi(\psi_j^{(i)}), \pi(v)) = c(\phi_j^{(i)}, \pi(v)), \quad \forall v \in V.$$

Then we define

$$W_{glo}^1 = \text{span}\{\psi_j^{(i)} \mid 1 \leq j \leq J_i, 1 \leq i \leq N\}. \quad (20)$$

To define the space W_{glo}^2 , we find $\eta_i \in V$ such that

$$a^*(\eta_i, v) + c(\pi(\eta_i), \pi(v)) = (q_i, v)_V - a(v, \xi_i), \quad \forall v \in V$$

where ξ_i is defined in (18). Then we define

$$W_{glo}^2 = \text{span}\{\eta_i + \xi_i \mid 1 \leq i \leq N_c\}. \quad (21)$$

Finally, we define $W_{glo} = W_{glo}^1 + W_{glo}^2$. Before we discuss our stability results, we will give a characterization of the space W_{glo}^1 in the following lemma.

Lemma 1. *Let W_{glo}^1 be the space defined in (20). Then, $u \in W_{glo}^1$ if and only if there is $\phi \in W_{aux}$ such that*

$$a^*(u, v) = c(\phi, v), \quad \forall v \in V. \quad (22)$$

Proof. First, we will define operators $L_1 : W_{aux} \rightarrow V$ and $L_2 : W_{aux} \rightarrow V$ such that for a given $v \in W_{aux}$, the images $L_1(v)$ and $L_2(v)$ are defined by solving the following equations

$$\begin{aligned} a^*(L_1(v), w) + c(\pi(L_1(v)), \pi(w)) &= c(v, w), \quad \forall w \in V, \\ a^*(L_2(v), w) &= c(v, w), \quad \forall w \in V. \end{aligned}$$

It is clear that $L_1(W_{aux}) \subset L_2(W_{aux})$, since for any $v \in W_{aux}$, we have

$$a^*(L_1(v), w) = c(v - \pi(L_1(v)), w), \quad \forall w \in V,$$

and therefore $L_1(v) = L_2(v - \pi(L_1(v)))$.

Next, we define the space \widehat{W}_{aux} as $\widehat{W}_{aux} = \{v \in W_{aux} \mid c(v, w) = 0 \text{ for all } w \in V\}$. The space \widetilde{W}_{aux} is then defined as the orthogonal complement of \widehat{W}_{aux} with respect to the c -inner product such that $W_{aux} = \widehat{W}_{aux} \oplus \widetilde{W}_{aux}$. Since W_{aux} is a finite dimensional vector space, we have

$$\dim(L_i(W_{aux})) + \dim(\ker(L_i)) = \dim(W_{aux}), \quad i = 1, 2.$$

Since $\ker(L_i) = \widehat{W}_{aux}$ for $i = 1, 2$, we have

$$\dim(L_i(W_{aux})) = \dim(W_{aux}) - \dim(\widehat{W}_{aux}) = \dim(\widetilde{W}_{aux}), \quad i = 1, 2,$$

which implies $\dim(L_1(W_{aux})) = \dim(L_2(W_{aux}))$. Hence, we obtain $L_1(W_{aux}) = L_2(W_{aux})$. This completes the proof. \square

Next, we define a norm

$$\|w\|_W = \sup_{v \in V} \frac{a(v, w)}{\|v\|_V}.$$

Lemma 2. *For all $w \in V$, we have*

$$\|w\|_W = \sqrt{r(w, w)}. \quad (23)$$

Proof. By the definition of T , we have

$$a(v, Tu) = (u, v)_V, \quad \forall v \in V.$$

Thus, by considering $w = Tu$, we have $a(v, w) = (T^{-1}w, v)_V$. Therefore, for all $w \in V$, we have

$$\|T^{-1}w\|_V^2 = a(T^{-1}w, w) \leq \|w\|_W \|T^{-1}w\|_V$$

and

$$\|w\|_W = \sup_{v \in V} \frac{a(v, w)}{\|v\|_V} = \sup_{v \in V} \frac{(T^{-1}w, v)_V}{\|v\|_V} \leq \|T^{-1}w\|_V.$$

Therefore, we have $\sqrt{r(w, w)} = \|T^{-1}w\|_V = \|w\|_W$. \square

Our first result regarding stability is Lemma 3. We consider the problem: find $(w, u) \in W_{glo} \times V_{ms}$ such that

$$\begin{aligned} r(w, z) + a(u, z) &= (f, z), \quad \forall z \in W_{glo}, \\ a^*(w, v) &= 0, \quad \forall v \in V_{ms}. \end{aligned}$$

The following lemma shows that the test space W_{glo} gives perfect stability.

Lemma 3. *For all $v \in V_{ms}$, there exist a unique $w \in W_{glo}$ such that*

$$(u, v)_V = a(u, w), \quad \forall u \in V. \quad (24)$$

Therefore we have

$$\inf_{v \in V_{ms}} \sup_{z \in W_{glo}} \frac{a(v, z)}{\|v\|_V \|z\|_W} = 1.$$

Proof. By definition of W_{glo}^2 , for each $q_i \in V_{ms}$, there exist a function $\eta_i + \xi_i \in W_{glo}^2$ such that

$$a^*(\eta_i + \xi_i, v) = (q, v)_V - c(\pi(\eta_i), v), \quad \forall v \in V.$$

On the other hand, by Lemma 1, there exist a function $w \in W_{glo}^1$ such that

$$a^*(w, v) = c(\pi(\eta_i), v), \quad \forall v \in V.$$

Therefore we have

$$a^*(\eta_i + \xi_i + w, v) = (q, v)_V, \quad \forall v \in V.$$

This completes the proof for (24). To show the second part, we note that (24) implies that for every $v \in V_{ms}$, there is $w \in W_{glo}$ such that

$$\|v\|_V^2 = a(v, w)$$

and that $\|w\|_W = \|v\|_V$. This shows the second part of the lemma. \square

We next prove a localization result for our test functions. In particular, we will prove a localization property for functions in W_{glo}^1 . First, we need some notations for the oversampling domain and the cutoff function with respect to these oversampling domains. For each K_i , we recall that $K_{i,m} \subset \Omega$ is the oversampling coarse region by enlarging K_i by m coarse grid layers. For $M > m$, we define $\chi_i^{M,m} \in \text{span}\{\chi_j^{ms}\}$ such that $0 \leq \chi_i^{M,m} \leq 1$ and

$$\chi_i^{M,m} = 1 \text{ in } K_{i,m}, \quad (25)$$

$$\chi_i^{M,m} = 0 \text{ in } \Omega \setminus K_{i,M}. \quad (26)$$

Note that, we have $K_{i,m} \subset K_{i,M}$. Moreover, $\chi_i^{M,m} = 1$ on the inner region $K_{i,m}$ and $\chi_i^{M,m} = 0$ outside the outer region $K_{i,M}$.

Lemma 4. *Let S be a given coarse region and let S_l be an oversampling region obtained by enlarging S by l coarse grid layers, where $l \geq 2$. Let $w_{glo} \in V$ be the solution of*

$$a^*(w_{glo}, v) + c(\pi(w_{glo}), \pi(v)) = L(v), \quad \forall v \in V,$$

where $L(v)$ is a linear functional such that $L(v) = 0, \forall v \in V_0(\Omega \setminus S)$. In addition, we let $w_{ms} \in V_0(S_l)$ be the solution of

$$a^*(w_{ms}, v) + c(\pi(w_{ms}), \pi(v)) = L(v), \quad \forall v \in V_0(S_l).$$

Then, we have

$$\|w_{glo} - w_{ms}\|_V^2 \leq C \left(1 + \Lambda^{-1}\right) \left(1 + C^{-1}(1 + \Lambda^{-1})^{-1}\right)^{-(l-1)} \|w_{glo}\|_V^2,$$

where $\Lambda = \min_{1 \leq i \leq N} \lambda_{J_{i+1}}^{(i)}$.

Proof. Using the definitions of w_{glo} and w_{ms} , we have

$$a^*(w_{glo} - w_{ms}, v) + c(\pi(w_{glo} - w_{ms}), \pi(v)) = 0$$

for all $v \in V_0(S_l)$. Therefore, for all $v \in V_0(S_l)$, we have

$$\begin{aligned} \|w_{glo} - w_{ms}\|_V^2 &= \left(a^*(w_{glo} - w_{ms}, w_{glo} - w_{ms}) + c(\pi(w_{glo} - w_{ms}), \pi(w_{glo} - w_{ms})) \right) \\ &= \left(a^*(w_{glo} - w_{ms}, w_{glo} - v) + c(\pi(w_{glo} - w_{ms}), \pi(w_{glo} - v)) \right) \end{aligned}$$

since $b(x)$ is divergence free. Choosing $v = \chi^{l,l-1}w_{glo}$, we have

$$\begin{aligned}
& a^*(w_{glo} - w_{ms}, (1 - \chi_i^{l,l-1})w_{glo}) \\
&= \int \kappa \nabla(w_{glo} - w_{ms}) \cdot \nabla((1 - \chi^{l,l-1})w_{glo}) + \int (w_{glo} - w_{ms})b \cdot \nabla((1 - \chi^{l,l-1})w_{glo}) \\
&\leq \left(\|w_{glo} - w_{ms}\|_{s(\Omega \setminus S_{l-1})} + \|w_{glo} - w_{ms}\|_{c(\Omega \setminus S_{l-1})} \right) \|(1 - \chi^{l,l-1})w_{glo}\|_{s(\Omega \setminus S_{l-1})} \\
&\leq C \left(\|w_{glo} - w_{ms}\|_{s(\Omega \setminus S_{l-1})} + \|w_{glo} - w_{ms}\|_{c(\Omega \setminus S_{l-1})} \right) \left(\|w_{glo}\|_{s(\Omega \setminus S_{l-1})} + \|\tilde{\kappa}^{\frac{1}{2}}w_{glo}\|_{L^2(\Omega \setminus S_{l-1})} \right)
\end{aligned}$$

and

$$\begin{aligned}
\|\pi((1 - \chi^{(l,l-1)})w_{glo})\|_{c(\Omega \setminus S_{l-1})}^2 &\leq \|(1 - \chi^{(l,l-1)})w_{glo}\|_{c(\Omega \setminus S_{l-1})}^2 \\
&= \|w_{glo}\|_{c(\Omega \setminus S_l)}^2 + \sum_{K_i \subset (S_i \setminus S_{i-1})} c^{(i)}((1 - \chi^{(l,l-1)})w_{glo}, (1 - \chi^{(l,l-1)})w_{glo}).
\end{aligned}$$

Next, we will estimate the term $c^{(i)}((1 - \chi^{(l,l-1)})w_{glo}, (1 - \chi^{(l,l-1)})w_{glo})$. By definition, we have

$$\begin{aligned}
c^{(i)}((1 - \chi^{(l,l-1)})w_{glo}, (1 - \chi^{(l,l-1)})w_{glo}) &= \int_{K_i} \left(\frac{|b|^2}{\kappa} + \tilde{\kappa} \right) |(1 - \chi^{(l,l-1)})w_{glo}|^2 \\
&\leq \int_{K_i} \left(\frac{|b|^2}{\kappa} + \tilde{\kappa} \right) |w_{glo}|^2 = c^{(i)}(w_{glo}, w_{glo}).
\end{aligned}$$

Thus we obtain

$$\|w_{glo} - w_{ms}\|_V^2 \leq C \left(\|w_{glo} - w_{ms}\|_{s(\Omega \setminus S_{l-1})} + \|w_{glo} - w_{ms}\|_{c(\Omega \setminus S_{l-1})} \right) \left(\|w_{glo}\|_{c(\Omega \setminus S_{l-1})} + \|w_{glo}\|_{s(\Omega \setminus S_{l-1})} \right).$$

Next we will estimate the terms $\|w_{glo}\|_{c(\Omega \setminus S_{l-1})}$ and $\|w_{glo} - w_{ms}\|_{c(\Omega \setminus S_{l-1})}$. We will divide the proof in 4 steps.

Step 1: For a given $u \in V$ and $K_i \in \mathcal{T}_H$, we have

$$\begin{aligned}
\|u\|_{c(K_i)}^2 &= \|\pi u\|_{c(K_i)}^2 + \|(I - \pi)u\|_{c(K_i)}^2 \\
&\leq \|\pi u\|_{c(K_i)}^2 + \frac{1}{\Lambda} \|u\|_{s(K_i)}^2 \\
&\leq (1 + \Lambda^{-1}) \|u\|_V^2(K_i).
\end{aligned}$$

Thus, we have

$$\|w_{glo} - w_{ms}\|_V \leq C(1 + \Lambda^{-1})^{\frac{1}{2}} \|w_{glo}\|_{V(\Omega \setminus S_{l-1})}. \quad (27)$$

Step 2: In this step, we will prove $\|w_{glo}\|_{V(\Omega \setminus S_k)} \leq C\|w_{glo}\|_{V(S_k \setminus S_{k-1})}$. By direct computations, we have

$$\int_{\Omega} \kappa \nabla w_{glo} \cdot \nabla(1 - \chi_i)w_{glo} = \|w_{glo}\|_{s(\Omega \setminus S_k)}^2 + \int_{S_k \setminus S_{k-1}} \kappa \nabla w_{glo} \cdot \nabla(1 - \chi_i)w_{glo}$$

and

$$\int_{\Omega} b \cdot \nabla w_{glo}(1 - \chi_i)w_{glo} = \frac{1}{2} \int_{\Omega \setminus S_{l-1}} (b \cdot \nabla w_{glo})(1 - \chi_i)w_{glo} - \frac{1}{2} \int_{\Omega \setminus S_{l-1}} b \cdot \nabla((1 - \chi_i)w_{glo})w_{glo}$$

and

$$c(\pi w_{glo}, \pi((1 - \chi_i)w_{glo})) = \|\pi(w_{glo})\|_{c(\Omega \setminus S_{k-1})}^2 + \sum_{K_i \subset S_k \setminus S_{k-1}} c^{(i)}(\pi w_{glo}, \pi((1 - \chi^{(k,k-1)})w_{glo})).$$

Using the above equations, we have

$$\begin{aligned}
\|w_{glo}\|_{V(\Omega \setminus S_k)}^2 &= - \int_{S_k \setminus S_{k-1}} \kappa \nabla w_{glo} \cdot \nabla (1 - \chi_i) w_{glo} \\
&\quad - \frac{1}{2} \left(\int_{S_i \setminus S_{i-1}} b \cdot \nabla w_{glo} (1 - \chi^{(k,k-1)}) w_{glo} - \int_{S_i \setminus S_{i-1}} b \cdot \nabla \left((1 - \chi^{(k,k-1)}) w_{glo} \right) w_{glo} \right) \\
&\quad - \sum_{K_i \subset S_k \setminus S_{k-1}} c^{(i)} (\pi w_{glo}, \pi \left((1 - \chi^{(k,k-1)}) w_{glo} \right)) \\
&= T_1 + T_2 + T_3.
\end{aligned}$$

Next, we will estimate the term T_1 . Clearly,

$$\begin{aligned}
\int_{S_k \setminus S_{k-1}} \kappa \nabla w_{glo} \cdot \nabla (1 - \chi^{(k,k-1)}) w_{glo} &\leq C \|w_{glo}\|_{s(S_k \setminus S_{k-1})} \left(\|w_{glo}\|_{s(S_k \setminus S_{k-1})} + \|w_{glo}\|_{c(S_k \setminus S_{k-1})} \right) \\
&\leq C(1 + \Lambda^{-1})^{\frac{1}{2}} \|w_{glo}\|_{V(S_k \setminus S_{k-1})} \|w_{glo}\|_{s(S_k \setminus S_{k-1})}.
\end{aligned}$$

Secondly, we will estimate the term T_2 . We have

$$\begin{aligned}
&-\frac{1}{2} \left(\int_{S_i \setminus S_{i-1}} (b \cdot \nabla w_{glo}) (1 - \chi^{(k,k-1)}) w_{glo} - \int_{S_i \setminus S_{i-1}} b \cdot \nabla \left((1 - \chi^{(k,k-1)}) w_{glo} \right) w_{glo} \right) \\
&\leq C \|w_{glo}\|_{s(S_k \setminus S_{k-1})} \left\| \frac{|b|}{\kappa^{\frac{1}{2}}} w_{glo} \right\|_{L^2(S_k \setminus S_{k-1})} + \left\| \left(\frac{|b|^2}{\kappa} \right)^{\frac{1}{2}} w_{glo} \right\|_{L^2(S_k \setminus S_{k-1})} \|\tilde{\kappa}^{\frac{1}{2}} w_{glo}\|_{L^2(S_k \setminus S_{k-1})} \\
&\leq C \left(\|w_{glo}\|_{s(S_k \setminus S_{k-1})} + \|w_{glo}\|_{c(S_k \setminus S_{k-1})} \right) \|w_{glo}\|_{c(S_k \setminus S_{k-1})}.
\end{aligned}$$

Finally, we will estimate the term T_3 . We have

$$\begin{aligned}
- \sum_{K_i \subset S_k \setminus S_{k-1}} c^{(i)} (\pi w_{glo}, \pi \left((1 - \chi^{(k,k-1)}) w_{glo} \right)) &\leq \|\pi w_{glo}\|_{c(S_k \setminus S_{k-1})} \|(1 - \chi^{(k,k-1)}) w_{glo}\|_{c(S_k \setminus S_{k-1})} \\
&\leq C(1 + \Lambda^{-1})^{\frac{1}{2}} \|\pi w_{glo}\|_{c(S_k \setminus S_{k-1})} \|w_{glo}\|_{V(S_k \setminus S_{k-1})}.
\end{aligned}$$

Combining the above results, we have

$$\|w_{glo}\|_{V(\Omega \setminus S_k)}^2 \leq C(1 + \Lambda^{-1}) \|w_{glo}\|_{V(S_k \setminus S_{k-1})}^2. \tag{28}$$

Step 3: In this step, we will prove that $\|w_{glo}\|_{V(\Omega \setminus S_k)} \leq (1 + C^{-1}(1 + \Lambda^{-1})^{-1})^{-1} \|w_{glo}\|_{V(S_k \setminus S_{k-1})}$. Indeed, we have

$$\begin{aligned}
\|w_{glo}\|_{V(\Omega \setminus S_{k-1})}^2 &= \|w_{glo}\|_{V(\Omega \setminus S_k)}^2 + \|w_{glo}\|_{V(S_k \setminus S_{k-1})}^2 \\
&\geq (1 + C^{-1}(1 + \Lambda^{-1})^{-1}) \|w_{glo}\|_{V(\Omega \setminus S_k)}^2
\end{aligned} \tag{29}$$

Step 4: In this step, we will prove the required estimate. Using (27), (28) and (29), we have

$$\begin{aligned}
\|w_{glo} - w_{ms}\|_{V}^2 &\leq C(1 + \Lambda^{-1}) \|w_{glo}\|_{V(\Omega \setminus S_{i-1})}^2 \\
&\leq C(1 + \Lambda^{-1}) (1 + C^{-1}(1 + \Lambda^{-1})^{-1})^{-(l-1)} \|w_{glo}\|_{V(\Omega \setminus S)}^2 \\
&\leq C(1 + \Lambda^{-1}) (1 + C^{-1}(1 + \Lambda^{-1})^{-1})^{-(l-1)} \|w_{glo}\|_{V}^2.
\end{aligned}$$

□

The following is the main result of this section. It states that our test space gives a stable numerical scheme.

Theorem 1. Assume that $N_d^{\frac{1}{2}}CED < 1$. For any given $u \in V_{ms}$, there exists a function $w \in W_{ms}$ such that

$$\frac{1 - N_d^{\frac{1}{2}}CED}{1 + N_d^{\frac{1}{2}}CED} \|u\|_V \leq \frac{a(u, w)}{\|w\|_W}$$

where $E = C(1 + \Lambda^{-1}) \left(1 + C^{-1}(1 + \Lambda^{-1})^{-1}\right)^{-(l-1)}$ is the same constant in Lemma 4, N_d is the maximum of numbers of coarse grid vertices and cells and $D = \kappa_0^{-1} \max\{\kappa^{-1}|b|^2, \tilde{\kappa}\}$.

Proof. Since $u \in V_{ms}$, we can write $u = \sum_{i=1}^{N_c} d_i q_i$ as a linear combination of trial basis functions $\{q_i\}$ in V_{ms} , where d_i are scalars. By Lemma 3, there exists a function $w_{glo} \in W_{glo}$ such that

$$(u, v)_V = a(v, w_{glo}), \quad \forall v \in V$$

and we can write

$$w_{glo} = w_1 + w_2$$

where

$$\begin{aligned} a^*(w_1, v) + c(\pi w_1, v) &= (u, v)_V, \quad \forall v \in V, \\ a^*(w_2, v) &= -c(\pi w_1, v), \quad \forall v \in V. \end{aligned}$$

Next, we define $w_1^{(i)} \in V$, $w_2^{(j)} \in V$ such that

$$\begin{aligned} a^*(w_1^{(i)}, v) + c(\pi w_1^{(i)}, v) &= (d_i q_i, v)_V, \quad \forall v \in V, \\ a^*(w_2^{(j)}, v) + c(\pi w_2^{(j)}, v) &= c^{(j)}((\pi w_2 - \pi w_1)|_{K_j}, v), \quad \forall v \in V \end{aligned}$$

and $w_{1,ms}^{(i)} \in W_{ms}$, $w_{2,ms}^{(j)} \in W_{ms}$ be the corresponding localized functions defined by

$$\begin{aligned} a^*(w_{1,ms}^{(i)}, v) + c(\pi w_{1,ms}^{(i)}, v) &= (d_i q_i, v)_V, \quad \forall v \in V_0(\omega_i^+), \\ a^*(w_{2,ms}^{(j)}, v) + c(\pi w_{2,ms}^{(j)}, v) &= c^{(j)}((\pi w_2 - \pi w_1)|_{K_j}, v), \quad \forall v \in V_0(K_j^+). \end{aligned}$$

Clearly, we have $w_{glo} = \sum_i w_1^{(i)} + \sum_j w_2^{(j)}$, where the index i corresponds to coarse vertices and the index j corresponds to coarse cells. We take $w = \sum_i w_{1,ms}^{(i)} + \sum_j w_{2,ms}^{(j)} \in W_{ms}$. Then we have the following

$$\begin{aligned} \|u\|_V^2 &= a(u, w_{glo}) = a(u, w_{glo} - w) + a(u, w) \\ &= \sum_i a(u, w_1^{(i)} - w_{1,ms}^{(i)}) + \sum_j a(u, w_2^{(j)} - w_{2,ms}^{(j)}) + a(u, w). \end{aligned} \quad (30)$$

Notice that, using Lemma 4, the first two terms on the right hand side of (30) can be estimated as follows

$$\begin{aligned} a(u, w_1^{(i)} - w_{1,ms}^{(i)}) &\leq C \|u\|_V \|w_1^{(i)} - w_{1,ms}^{(i)}\|_V \\ &\leq CE \|u\|_V \|d_i q_i\|_V \end{aligned}$$

and

$$\begin{aligned} a(u, w_2^{(j)} - w_{2,ms}^{(j)}) &\leq C \|u\|_V \|w_2^{(j)} - w_{2,ms}^{(j)}\|_V \\ &\leq CE \|u\|_V \|(\pi w_2 - \pi w_1)|_{K_j}\|_c \end{aligned}$$

where the c -norm is defined as $\|w\|_c^2 = c(w, w)$. Therefore, the first two terms on the right hand side of (30) can be estimated as

$$\sum_i a(u, w_1^{(i)} - w_{1,ms}^{(i)}) + \sum_j a(u, w_2^{(j)} - w_{2,ms}^{(j)}) \leq N_d^{\frac{1}{2}} CE \|u\|_V \left(\left(\sum_i d_i^2 \|q_i\|_V^2 \right)^{\frac{1}{2}} + \|(\pi w_2 - \pi w_1)\|_c \right).$$

Notice that, by the Poincare inequality, we have

$$\|w_2\|_c \leq CD\|w_2\|_s.$$

By the definition of w_2 , we have $\|w_2\|_s \leq C\|w_1\|_c$, and by the definition of w_1 , we have $\|w_1\|_c \leq C\|u\|_V$. Furthermore, by the assumption on stable decomposition (7), we have $(\sum d_i^2 \|q_i\|_V^2)^{\frac{1}{2}} \leq C_s \|\sum_i d_i q_i\|_V$. Thus we have

$$\begin{aligned} \sum_i a(u, w_1^{(i)} - w_{1,ms}^{(i)}) + \sum_j a(u, w_2^{(j)} - w_{2,ms}^{(j)}) &\leq N_d^{\frac{1}{2}} CED \|u\|_V \left(\|\sum_i d_i q_i\|_V + \|\pi w_2\|_c + \|\pi w_1\|_c \right) \\ &\leq N_d^{\frac{1}{2}} CED \|u\|_V^2. \end{aligned}$$

Similarly, for all $v \in V_{ms}$, we have

$$a(v, w_{glo} - w) \leq N_d^{\frac{1}{2}} CED \|u\|_V \|v\|_V.$$

Finally, we have

$$\begin{aligned} \frac{a(u, w)}{\|w\|_W} &\geq \frac{a(u, w - w_{glo}) + a(u, w_{glo})}{\|w_{glo}\|_W + \|w - w_{glo}\|_W} \\ &\geq \frac{1 - N_d^{\frac{1}{2}} CED}{1 + N_d^{\frac{1}{2}} CED} \|u\|_V \end{aligned}$$

for $N_d^{\frac{1}{2}} CED < 1$. This completes the proof. \square

In the above theorem, we assume that $N_d^{\frac{1}{2}} CED < 1$. This can be achieved by using large enough number of layers l in the construction of oversampling layers in the definitions of test spaces (17) and (19).

4 Numerical results

In this section, we will present some numerical examples to demonstrate the performance of the method. For the following example, we consider $h = 1/200$ and $\Omega = [0, 1]^2$. We will show the performance by considering various coarse grid sizes and number of oversampling layers. We notice that the number of test functions in the space W_{ms}^1 depends on the number of eigenfunctions selected in the auxiliary spectral problem. Thus, we will consider various choices of this number and show that one needs to include enough eigenfunctions to obtain stability. For the space W_{ms}^2 , its dimension depends on the number of trial basis functions. In our simulations, we choose piecewise linear functions as our trial basis.

We next discuss some implementation details. We use A to denote a fine scale discretization of the original problem (5). We use the matrix Q to represent the matrix representation of the trial basis functions, and the matrix W to represent the matrix representation of the test functions. In addition, we use the matrix V to denote the matrix representation of the inner product $(\cdot, \cdot)_V$. Then the matrix form of (14)-(15) is given by

$$\begin{aligned} W^T A V^{-1} A^T W \vec{w} + W^T A Q \vec{u} &= W^T F \\ Q^T A^t W \vec{w} &= 0 \end{aligned} \tag{31}$$

where \vec{u} and \vec{w} denote the vector representations of u and w , and F is the vector representation of f . We observe that (31) contains the matrix V^{-1} . In simulations, we will replace V^{-1} by the matrix B^{-1} where B is the matrix representation of the inner product $c(\cdot, \cdot)$, where c is defined in (9), and can be diagonalized by mass lumping. The motivation of this replacement is that the norm induced by $s^{(i)}$, defined in (8), can be

controlled by the norm induced by $c^{(i)}$ in the discrete case under an assumption. Notice that, by the inverse inequality, we have

$$s^{(i)}(u, u) \leq Ch^{-2} \left(\max_{x \in K_i} \frac{\kappa(x)}{|b(x)|} \right)^2 c^{(i)}(u, u),$$

where h is the fine mesh size. Thus, if we assume the fine mesh size satisfies $h^{-1} \left(\max_{x \in K_i} \frac{\kappa(x)}{|b(x)|} \right) = O(1)$, then we have the desired replacement.

4.1 Example 1

In our first example, we consider a constant diffusion coefficient, that is, $\kappa = 1/200$. The velocity field is given by $b = (\cos(18\pi y) \sin(18\pi x), -\cos(18\pi x) \sin(18\pi y))$ and the source term is given by $f = 1$. The numerical results are shown in Table 1. In the first column, we present the number of test functions used for the space W_{ms}^1 per coarse element. The second column shows the coarse mesh size, and the third column shows the number of oversampling layers used in the constructions of test functions for both W_{ms}^1 and W_{ms}^2 . Finally, in the last column, we present the relative errors in the V -norm. For comparison purpose, we show the projection errors in V -norm in parenthesis, where the projection error is obtained by projecting the true solution in the trial space using the V -inner product. From the results in Table 1, we observe that the error is close to the projection error once sufficient oversampling layers are used in the construction of test functions.

#basis(W_{ms}^1)	H	#layer	V -norm (projection error)
3	1/10	3	3.05%(2.92%)
3	1/20	4	2.19%(2.18%)
3	1/40	5	0.85%(0.85%)

Table 1: Numerical results for Example 1.

4.2 Example 2

In our second example, we perform a similar test as in Example 1, but we use $\kappa = 1/2000$ and $b = (-\partial_y H, +\partial_x H)$, where $H = (\sin(5\pi x) \sin(6\pi y) / (60\pi)) + 0.005(x + y)$. In this case, the Peclet number is larger than that of Example 1. The numerical results are shown in Table 2. We observe similar performance as in Example 1.

#basis(W_{ms}^1)	H	#layer	V -norm (projection error)
3	1/10	3	11.79%(11.07%)
3	1/20	4	3.25%(3.24%)
3	1/40	5	0.69%(0.68%)

Table 2: Numerical results for Example 2.

4.3 Example 3

Finally, we consider a heterogenous velocity field defined by a Darcy flow in a high contrast medium. In particular, the velocity b is defined by the following system

$$\begin{aligned} K^{-1}b &= -\nabla p \\ \nabla \cdot b &= q \end{aligned}$$

where

$$q(x) = \begin{cases} 1 & x \in [0, \frac{1}{10}] \times [0, \frac{1}{10}] \\ -1 & x \in [\frac{9}{10}, 1] \times [\frac{9}{10}, 1] \\ 0 & \text{otherwise} \end{cases}$$

and

$$f(x) = \begin{cases} 1 & x \in [0, \frac{1}{10}] \times [0, \frac{1}{10}] \\ 0 & \text{otherwise} \end{cases}$$

and the coefficient K is shown in Figure 2, where the contrast is 10^4 . In addition, we take $\kappa = 1/20$. The numerical results are presented in Table 3. We observe that the solution error is very close to the projection error once a sufficient number of oversampling layers is used in the construction of test functions. This result confirm that our test space gives very good stability, even for high Peclet numbers.

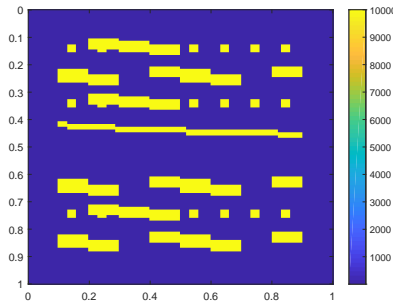


Figure 2: The coefficient K for Example 3.

#basis(W_{ms}^1)	H	#layer	V -norm (projection error)
3	1/10	3	16.16%(15.86%)
3	1/20	4	4.61%(4.59%)
3	1/40	5	1.20%(1.20%)

Table 3: Numerical results for Example 3.

5 Conclusion

We have presented a new stabilization technique for multiscale convection diffusion problems. The proposed methodology is based on the DPG idea with a suitable choice of test functions. The construction of the test function is based on the CEM-GMsFEM approach. We show that, once a sufficient number of oversampling layers is used, the resulting test functions have a decay property, and give a good stability. We also present numerical results to confirm this theory.

References

- [1] I Akkerman, Y Bazilevs, VM Calo, TJR Hughes, and S Hulshoff. The role of continuity in residual-based variational multiscale modeling of turbulence. *Computational Mechanics*, 41(3):371–378, 2008.

- [2] M Alotaibi, VM Calo, Y Efendiev, JC Galvis, and M Ghommem. Global–local nonlinear model reduction for flows in heterogeneous porous media. *Computer Methods in Applied Mechanics and Engineering*, 292:122–137, 2015.
- [3] T. Arbogast. Analysis of a two-scale, locally conservative subgrid upscaling for elliptic problems. *SIAM J. Numer. Anal.*, 42(2):576–598 (electronic), 2004.
- [4] JW Barrett and KW Morton. Approximate symmetrization and Petrov-Galerkin methods for diffusion-convection problems. *Computer Methods in Applied Mechanics and Engineering*, 45(1):97–122, 1984.
- [5] Y Bazilevs, VM Calo, JA Cottrell, TJR Hughes, A Reali, and G Scovazzi. Variational multiscale residual-based turbulence modeling for large eddy simulation of incompressible flows. *Computer Methods in Applied Mechanics and Engineering*, 197(1):173–201, 2007.
- [6] Y Bazilevs, C Michler, VM Calo, and TJR Hughes. Isogeometric variational multiscale modeling of wall-bounded turbulent flows with weakly enforced boundary conditions on unstretched meshes. *Computer Methods in Applied Mechanics and Engineering*, 199(13):780–790, 2010.
- [7] PB Bochev and MD Gunzburger. Finite element methods of least-squares type. *SIAM review*, 40(4):789–837, 1998.
- [8] PB Bochev and MD Gunzburger. *Least-squares finite element methods*, volume 166. Springer Science & Business Media, 2009.
- [9] A Buffa, TJR Hughes, and G Sangalli. Analysis of a multiscale discontinuous Galerkin method for convection-diffusion problems. *SIAM Journal on Numerical Analysis*, 44(4):1420–1440, 2006.
- [10] VM Calo, Y Efendiev, J Galvis, and M Ghommem. Multiscale empirical interpolation for solving nonlinear PDEs. *Journal of Computational Physics*, 278:204–220, 2014.
- [11] VM Calo, Y Efendiev, J Galvis, and G Li. Randomized oversampling for generalized multiscale finite element methods. <http://arxiv.org/pdf/1409.7114.pdf>, 2014.
- [12] VM Calo, Y Efendiev, and JC Galvis. A note on variational multiscale methods for high-contrast heterogeneous porous media flows with rough source terms. *Advances in Water Resources*, 34(9):1177–1185, 2011.
- [13] VM Calo, Y Efendiev, and JC Galvis. Asymptotic expansions for high-contrast elliptic equations. *Mathematical Models and Methods in Applied Sciences*, 24(03):465–494, 2014.
- [14] J Chan, N Heuer, T Bui-Thanh, and L Demkowicz. A robust DPG method for convection-dominated diffusion problems ii: Adjoint boundary conditions and mesh-dependent test norms. *Computers & Mathematics with Applications*, 67(4):771–795, 2014.
- [15] F. Chen, E. Chung, and L. Jiang. Least-squares mixed generalized multiscale finite element method. *Computer Methods in Applied Mechanics and Engineering*, 311:764–787, 2016.
- [16] C.-C. Chu, I. G. Graham, and T.-Y. Hou. A new multiscale finite element method for high-contrast elliptic interface problems. *Math. Comp.*, 79(272):1915–1955, 2010.
- [17] Eric T Chung, Yalchin Efendiev, and Wing Tat Leung. An adaptive generalized multiscale discontinuous galerkin method (GMsDGM) for high-contrast flow problems. *arXiv preprint arXiv:1409.3474*, 2014.
- [18] Eric T Chung, Yalchin Efendiev, and Wing Tat Leung. Constraint energy minimizing generalized multiscale finite element method. *arXiv preprint arXiv:1704.03193*, 2017.
- [19] ET Chung, Y Efendiev, and WT Leung. Residual-driven online generalized multiscale finite element methods. *To appear in J. Comput. Phys.*

- [20] ET Chung, Y Efendiev, and WT Leung. An online generalized multiscale discontinuous Galerkin method (GMsDGM) for flows in heterogeneous media. *arXiv preprint arXiv:1504.04417*, 2015.
- [21] ET Chung, Y Efendiev, and G Li. An adaptive GMsFEM for high-contrast flow problems. *Journal of Computational Physics*, 273:54–76, 2014.
- [22] ET Chung, Y Efendiev, G Li, and M Vasilyeva. Generalized multiscale finite element methods for problems in perforated heterogeneous domains. *Applicable Analysis*, to appear, 2015.
- [23] R Codina. Comparison of some finite element methods for solving the diffusion-convection-reaction equation. *Computer Methods in Applied Mechanics and Engineering*, 156(1):185–210, 1998.
- [24] L Demkowicz and J Gopalakrishnan. A primal DPG method without a first-order reformulation. *Computers & Mathematics with Applications*, 66(6):1058–1064, 2013.
- [25] L Demkowicz, J Gopalakrishnan, and AH Niemi. A class of discontinuous Petrov-Galerkin methods. Part III: adaptivity. *Applied numerical mathematics*, 62(4):396–427, 2012.
- [26] L Demkowicz and N Heuer. Robust DPG method for convection-dominated diffusion problems. *SIAM Journal on Numerical Analysis*, 51(5):2514–2537, 2013.
- [27] L Demkowicz and JT Oden. An adaptive characteristic Petrov-Galerkin finite element method for convection-dominated linear and nonlinear parabolic problems in two space variables. *Computer Methods in Applied Mechanics and Engineering*, 55(1):63–87, 1986.
- [28] LF Demkowicz and J Gopalakrishnan. An overview of the discontinuous Petrov Galerkin method. In *Recent Developments in Discontinuous Galerkin Finite Element Methods for Partial Differential Equations*, pages 149–180. Springer International Publishing, 2014.
- [29] L.J. Durlofsky. Numerical calculation of equivalent grid block permeability tensors for heterogeneous porous media. *Water Resour. Res.*, 27:699–708, 1991.
- [30] W. E and B. Engquist. Heterogeneous multiscale methods. *Comm. Math. Sci.*, 1(1):87–132, 2003.
- [31] Y. Efendiev and J. Galvis. Coarse-grid multiscale model reduction techniques for flows in heterogeneous media and applications. *Chapter of Numerical Analysis of Multiscale Problems, Lecture Notes in Computational Science and Engineering, Vol. 83*, pages 97–125.
- [32] Y. Efendiev, J. Galvis, and T. Hou. Generalized multiscale finite element methods. *Journal of Computational Physics*, 251:116–135, 2013.
- [33] Y. Efendiev, J. Galvis, S. Ki Kang, and R.D. Lazarov. Robust multiscale iterative solvers for nonlinear flows in highly heterogeneous media. *Numer. Math. Theory Methods Appl.*, 5(3):359–383, 2012.
- [34] Y Efendiev, J Galvis, R Lazarov, M Moon, and M Sarkis. Generalized multiscale finite element method. Symmetric interior penalty coupling. *Journal of Computational Physics*, 255:1–15, 2013.
- [35] Y Efendiev, J Galvis, G Li, and M Presho. Generalized multiscale finite element methods. Oversampling strategies. *International Journal for Multiscale Computational Engineering*, accepted, 2013.
- [36] Y. Efendiev, J. Galvis, and X.H. Wu. Multiscale finite element methods for high-contrast problems using local spectral basis functions. *Journal of Computational Physics*, 230:937–955, 2011.
- [37] Y. Efendiev and T. Hou. *Multiscale Finite Element Methods: Theory and Applications*. Springer, 2009.
- [38] Y. Efendiev, T. Hou, and V. Ginting. Multiscale finite element methods for nonlinear problems and their applications. *Comm. Math. Sci.*, 2:553–589, 2004.

- [39] A Fannjiang and G Papanicolaou. Convection enhanced diffusion for periodic flows. *SIAM Journal on Applied Mathematics*, 54(2):333–408, 1994.
- [40] J Galvis and Y Efendiev. Domain decomposition preconditioners for multiscale flows in high-contrast media. *Multiscale Model. Simul.*, 8(4):1461–1483, 2010.
- [41] J Galvis and Y Efendiev. Domain decomposition preconditioners for multiscale flows in high contrast media: reduced dimension coarse spaces. *Multiscale Model. Simul.*, 8(5):1621–1644, 2010.
- [42] J Galvis, G Li, and K Shi. A generalized multiscale finite element method for the Brinkman equation. *Journal of Computational and Applied Mathematics*, 280:294–309, 2015.
- [43] J. Galvis and J. Wei. Ensemble level multiscale finite element and preconditioner for channelized systems and applications. *Journal of Computational and Applied Mathematics*, 255:456–467, 2014.
- [44] M. Ghommam, M. Presho, V. M. Calo, and Y. Efendiev. Mode decomposition methods for flows in high-contrast porous media. global-local approach. *Journal of Computational Physics*, 253:226–238, 2013.
- [45] M-C Hsu, Y Bazilevs, VM Calo, TE Tezduyar, and TJR Hughes. Improving stability of stabilized and multiscale formulations in flow simulations at small time steps. *Computer Methods in Applied Mechanics and Engineering*, 199(13):828–840, 2010.
- [46] TJR Hughes. Multiscale phenomena: Green’s functions, the Dirichlet-to-Neumann formulation, subgrid scale models, bubbles and the origins of stabilized methods. *Computer methods in applied mechanics and engineering*, 127(1):387–401, 1995.
- [47] TJR Hughes, VM Calo, and G Scovazzi. Variational and multiscale methods in turbulence. In *Mechanics of the 21st Century*, pages 153–163. Springer, 2005.
- [48] TJR Hughes, G Feijoo, L Mazzei, and J Quincy. The variational multiscale method—a paradigm for computational mechanics. *Comput. Methods Appl. Mech. Engrg.*, 166:3–24, 1998.
- [49] TJR Hughes, LP Franca, and GM Hulbert. A new finite element formulation for computational fluid dynamics: VIII. The Galerkin/least-squares method for advective-diffusive equations. *Computer Methods in Applied Mechanics and Engineering*, 73(2):173–189, 1989.
- [50] TJR Hughes and G Sangalli. Variational multiscale analysis: the fine-scale Green’s function, projection, optimization, localization, and stabilized methods. *SIAM Journal on Numerical Analysis*, 45(2):539–557, 2007.
- [51] G. Li, D. Peterseim, and M. Schedensack. Error analysis of a variational multiscale stabilization for convection-dominated diffusion equations in two dimensions. *IMA Journal of Numerical Analysis*, 2017.
- [52] A Masud and RA Khurram. A multiscale/stabilized finite element method for the advection–diffusion equation. *Computer Methods in Applied Mechanics and Engineering*, 193(21):1997–2018, 2004.
- [53] AH Niemi, NO Collier, and VM Calo. Discontinuous Petrov-Galerkin method based on the optimal test space norm for one-dimensional transport problems. *Procedia Computer Science*, 4:1862–1869, 2011.
- [54] AH Niemi, NO Collier, and VM Calo. Automatically stable discontinuous Petrov-Galerkin methods for stationary transport problems: Quasi-optimal test space norm. *Computers & Mathematics with Applications*, 66(10):2096–2113, 2013.
- [55] PJ Park and TY Hou. Multiscale numerical methods for singularly perturbed convection-diffusion equations. *International Journal of Computational Methods*, 1(01):17–65, 2004.

- [56] X.H. Wu, Y. Efendiev, and T.Y. Hou. Analysis of upscaling absolute permeability. *Discrete and Continuous Dynamical Systems, Series B.*, 2:158–204, 2002.
- [57] J Zitelli, I Muga, L Demkowicz, J Gopalakrishnan, D Pardo, and VM Calo. A class of discontinuous Petrov-Galerkin methods. Part IV: The optimal test norm and time-harmonic wave propagation in 1d. *Journal of Computational Physics*, 230(7):2406–2432, 2011.